

Influence of microstructure on the properties of $\text{Sr}_{0.5}\text{Pb}_{0.5}\text{TiO}_3$ V-shaped PTCR

Jingchang Zhao*, Longtu Li, Zhilun Gui

*State Key Laboratory of New Ceramics and Fine Processing, Department of Materials Science and Engineering,
Tsinghua University, Beijing 100084, PR China*

Received 12 January 2001; received in revised form 28 August 2001; accepted 24 September 2001

Abstract

Lanthanum-doped $\text{Sr}_{0.5}\text{Pb}_{0.5}\text{TiO}_3$ semiconducting ceramics were prepared by the solid state reaction technique with excess PbO additive. Samples' resistivities rise about 5 orders of magnitude above the Curie temperature ($T_c \approx 115^\circ\text{C}$) and their negative temperature coefficient of resistivity (NTCR) increases with an increase of the sintering temperature. The crystalline structure, microstructure and compositional distribution were investigated using XRD, scanning electron microscopy (SEM) and transmission electron microscopy (TEM) with X-ray energy dispersive analyses (EDAX), respectively. The distribution of Pb, Sr and Ti in the grain boundary layer has been shown to be similar to that in the grain interior. It is assumed that the PbO additive compensates Pb loss and keeps the Pb/Ti ratio stable in the grain boundary layers, which results in the low room temperature resistivity and weak NTCR effects. © 2002 Elsevier Science Ltd and Techna S.r.l. All rights reserved.

Keywords: $\text{Sr}_x\text{Pb}_{1-x}\text{TiO}_3$ thermistors; PTCR–NTCR effects

1. Introduction

In 1988, the V-shaped PTC effect was firstly found in $\text{Sr}_x\text{Pb}_{1-x}\text{TiO}_3$ ceramics [1]. With the elevating temperature, the resistivity of $\text{Sr}_x\text{Pb}_{1-x}\text{TiO}_3$ ceramics decreases sharply at $T < T_c$ and abruptly increases at $T > T_c$. These thermal sensitive ceramics can be sintered at a relatively low temperature and their Curie temperatures can move by changing the Pb/Sr ratios [2,3]. Owing to the novel NTC–PTC composite effects and relatively high resistivities at room temperature, $\text{Sr}_x\text{Pb}_{1-x}\text{TiO}_3$ semiconducting ceramics can be used in many fields, such as temperature control, self-regulating heaters as well as protection devices to reduce the damage to the main electrical components due to overflow at start-up [4].

Heywang model [5] was widely accepted to describe the conduction mechanism of $\text{Sr}_x\text{Pb}_{1-x}\text{TiO}_3$ -based ceramics in the PTC effect region. It was suggested that the acceptor states concentrate in the grain boundary to form a barrier, whose height can be increased rapidly near Curie temperature owing to the tetragonal to cubic phase transformation. As to the novel NTCR behavior below T_c , some attempts, such as the deep donor energy level [6], the

grain boundary effect [7] and the core–shell microstructure model [8,9] have been proposed to explain the strong NTC effect of $\text{Sr}_x\text{Pb}_{1-x}\text{TiO}_3$ V-shaped PTCR. However, some experimental phenomena still can not be satisfactorily interpreted.

Wang et al. [10] prepared low resistivity $\text{Sr}_x\text{Pb}_{1-x}\text{TiO}_3$ PTCR using chemical synthesis and rapid thermal sintering (RTS) processing and suggested that the NTC–PTC composite effects were originated from the grain boundary associated with complex impedance analyses [7]. However, the influences of defects and compositional distribution on the NTC behavior are still unclear. It is necessary to study the microstructure of the grain boundary layer, in depth, to reveal the conduction mechanism of $\text{Sr}_x\text{Pb}_{1-x}\text{TiO}_3$ semiconducting ceramics. In this article, $\text{Sr}_{0.5}\text{Pb}_{0.5}\text{TiO}_3$ V-shaped PTCR with different NTC effects were prepared at different sintering temperatures. The influence of excess PbO on the microstructure and compositional distribution was investigated.

2. Experimental

Stoichiometric powders of analytical grade PbO, TiO_2 and high purity SrTiO_3 (decomposed $\text{SrTiO}(\text{C}_2\text{O}_4)_2 \cdot 4\text{H}_2\text{O}$ at 1000°C for 4 h, produced in Xingtai, PR China)

* Corresponding author. Tel.: +86-10-62784579.

E-mail address: zhaojingchang99@mails.tsinghua.edu.cn (J. Zhao).

were accurately mixed and then calcinated at 800 °C for 2 h to prepare $\text{Sr}_{0.5}\text{Pb}_{0.5}\text{TiO}_3$ powders. Subsequently, 0.2–0.8 mol% $\text{La}(\text{NO}_3)_3$ solution and 0–4 mol% PbO were added to the $\text{Sr}_{0.5}\text{Pb}_{0.5}\text{TiO}_3$ powders and wet-milled in ethanol for 48 h in a plastic jar. After drying and sifting, the powders were pressed into disks with 10 mm diameter and about 1 mm thickness at a pressure of 200 MPa, then the green pellets were sintered at 1075–1150 °C for 1 h in air and cooled at the rate of 4 °C/min.

The surfaces of samples were rubbed with an In–Ga alloy and the resistivity-temperature characteristics were measured from room temperature up to 400 °C with a dc resistance-temperature measuring system. Phase structure and morphology were examined by X-ray diffraction (Regaku D/max IIIB) and SEM (JSM-6301F) respectively. After ion-beam thinning, the sample's micro-structure and compositional distribution were investigated by TEM (Hitachi-800) and EDAX (H-9100).

3. Results

The phase structure of the sintered $\text{Sr}_{0.5}\text{Pb}_{0.5}\text{TiO}_3$ ceramics is shown in Fig. 1. The samples have typical tetragonal crystal structure at room temperature with a c/a ratio of about 1.009.

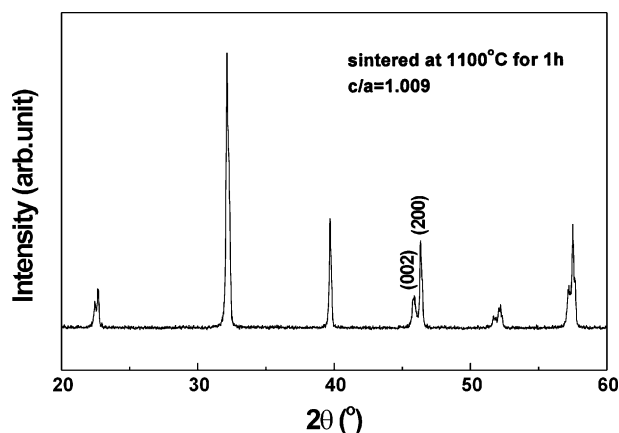


Fig. 1. The XRD patterns of $\text{Sr}_{0.5}\text{Pb}_{0.5}\text{TiO}_3$ ceramics.

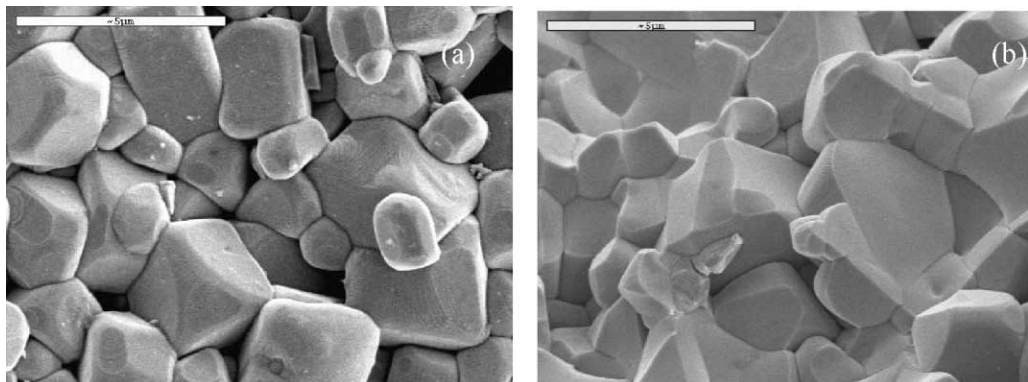


Fig. 2. SEM micrographs of $\text{Sr}_{0.5}\text{Pb}_{0.5}\text{TiO}_3$ ceramics: (a) surface, (b) fracture.

Fig. 2 gives the surface and fracture morphologies of an 1100 °C-1 h-sintered sample. It shows that the sizes of most grains are in the range of 2–5 μm and there are not any pores in the bulk. The sintered ceramics mainly fracture along the grain boundaries, showing that the mechanical strength of grains is higher than that of grain boundaries.

Fig. 3 shows the resistivity-temperature curves of the sintered samples at 1075, 1100, 1125 and 1150 °C for 1 h respectively. At $T > T_c$, it can be seen that all samples exhibit strong PTCR effects. The resistivity of sample 1 or 2 jumps more than 5 orders of magnitude and more than 4.5 orders corresponding to that of sample 3 or 4. The temperature of maximum resistivity in the PTCR effect region decreases with the raise of the sintering temperature. At $T < T_c$, the sintered samples have the minimum room temperature resistivity (ρ_{RT}) at 1100 °C. The variation of resistivity $\log(\rho_{RT}/\rho_{min})$ increases with

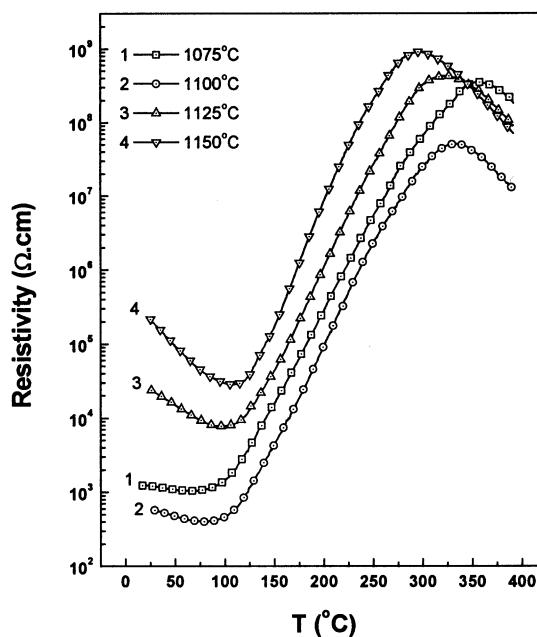


Fig. 3. Resistivity-temperature plots of La-doped $\text{Sr}_{0.5}\text{Pb}_{0.5}\text{TiO}_3$ ceramics sintered at 1075–1150 °C for 1 h.

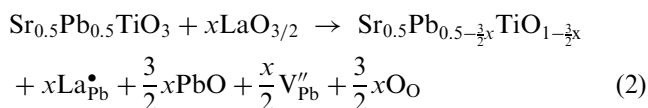
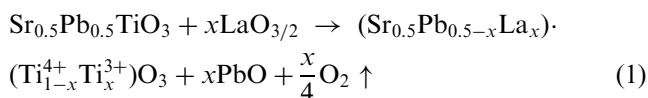
the raise of the sintering temperature, being ρ_{\min} the minimum resistivity of the sample at the measurement temperature. The NTC effect of samples 1 and 2 almost disappears, but samples 3 and 4 show a strong NTC effect below T_c .

A TEM micrograph of La-doped $\text{Sr}_{0.5}\text{Pb}_{0.5}\text{TiO}_3$ ceramics is shown in Fig. 4(a). It can be seen that the sintered samples have 90° domain structures inside the grains and discontinuous domain distribution through the grain boundaries. This microstructure is beneficial to stress release during phase transformation.

The distribution of Pb, Sr, Ti species in the grain interior and the grain boundary layer of 1100 °C-1 h sintered sample was measured by EDAX. Fig. 4(b) shows the peak intensities corresponding to Pb, Sr, Ti species in the grain interior to be similar to that in the grain boundary layer. Excess PbO is beneficial to suppress the formation of Pb-deficient grain boundary layer. The above result confirms the views in the literature [11] that the conventional sintered $\text{Sr}_x\text{Pb}_{1-x}\text{TiO}_3$ ceramics contain Pb-deficient grain boundary layers.

4. Discussion

According to defect chemistry, Sr or Pb positions in crystalline $\text{Sr}_{0.5}\text{Pb}_{0.5}\text{TiO}_3$ can be substituted by trivalent La^{3+} ions to form $\text{La}_{\text{Pb}}^\bullet$ or $\text{La}_{\text{Sr}}^\bullet$ defects. At the same time, PbO is easy to be lost into air during calcination [3,4,11], which will be beneficial to the substitution of Pb positions in $\text{Sr}_{0.5}\text{Pb}_{0.5}\text{TiO}_3$ lattices for La^{3+} ions. The reaction processes can be approximately described as follow:



In Eq. (1), the $\text{La}_{\text{Pb}}^\bullet$ defects produce residual charges in $\text{Sr}_{0.5}\text{Pb}_{0.5}\text{TiO}_3$ lattices that force tetravalent Ti^{4+} to reduce to trivalent Ti^{3+} . PbO loss makes the Eq. (1) move to the right, which increases the charge carrier density and improves the electrical conduction of $\text{Sr}_{0.5}\text{Pb}_{0.5}\text{TiO}_3$. However, PbO loss also make Eq. (2) move to the right and produce more V_{Pb}'' cationic vacancies to compensate $\text{La}_{\text{Pb}}^\bullet$, which decreases the charge carrier density and degenerate the electrical conduction of $\text{Sr}_{0.5}\text{Pb}_{0.5}\text{TiO}_3$ materials. Furthermore, overmuch PbO impurities concentrating on the grain boundaries force Eqs. (1) and (2) move to the left, which will suppress the production of electron carriers and V_{Pb}'' simultaneously. Therefore controlling Pb volatilization or supplying suitable PbO are key processes for preparing low resistivity $\text{Sr}_x\text{Pb}_{1-x}\text{TiO}_3$ ceramics. The above reasonably explains the experimental results in Fig. 3, i.e. the lowest room temperature resistivity showed by the 1100 °C-1 h sintered sample.

A core-shell microstructure was reported in microwave-sintered and rapid thermal sintered $\text{Sr}_x\text{Pb}_{1-x}\text{TiO}_3$ ceramics [6,7], the Pb-deficient core being packed by the Pb-rich $\text{Sr}_x\text{Pb}_{1-x}\text{TiO}_3$ perovskite and the electrical behavior of the core being completely shielded. The thickness of the shell varies with the temperature below the Curie

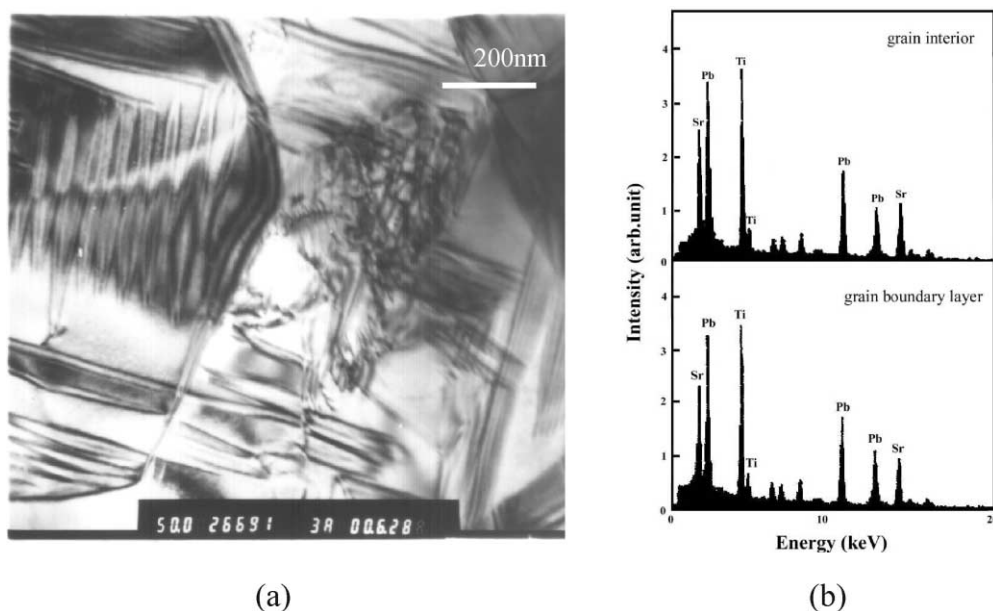


Fig. 4. (a) TEM micrograph and (b) EDAX spectra of the grain interior and the grain boundary layer of La-doped $\text{Sr}_{0.5}\text{Pb}_{0.5}\text{TiO}_3$ ceramics sintered at 1100 °C for 1 h with excess 2 mol% PbO.

temperature, which results in a large NTC effect. In our experiments, excess PbO impurities form a concentration gradient between the grain boundary layer and the grain interior during calcination. To some extent, the concentration gradient decreases the transfer of Pb^{2+} and prevents the formation of the Pb-deficient grain boundary layers. Therefore the core-shell microstructure was not observed in samples with PbO additive.

In general, PbO loss of samples increases at higher sintering temperature. Consequently much of Pb^{2+} vacancies are produced in the Pb-deficient grain boundary layers because oxygen atoms re-enter into $\text{Sr}_x\text{Pb}_{1-x}\text{TiO}_3$ crystal lattices during cooling. Pb^{2+} vacancies will combine partially with $\text{La}_{\text{Pb}}^\bullet$ donor defects to form defect complexes ($2\text{La}_{\text{Pb}}^\bullet \cdot \text{V}_{\text{Pb}}''$). These defect complexes in the grain boundary layers restrict the neighboring Ti^{4+} ions to accept electrons and participate in electrical conduction, which results in high room temperature resistivity and strong NTC effects below the Curie temperature.

5. Conclusions

La-doped $\text{Sr}_{0.5}\text{Pb}_{0.5}\text{TiO}_3$ V-shaped positive temperature coefficient resistors were prepared below 1150 °C by a conventional solid state reaction technique. The NTC effects of $\text{Sr}_{0.5}\text{Pb}_{0.5}\text{TiO}_3$ V-shaped PTCR ($T < T_c$) increase with the rise of the sintering temperature. Addition of PbO suppresses the migration of Pb ions in the grains and prevent the formation of Pb-deficient grain boundary layers, which results in low room temperature resistivities and weak NTC effects below the Curie temperature. It is assumed that the strong NTC effect of $\text{Sr}_x\text{Pb}_{1-x}\text{TiO}_3$ semiconducting ceramics is closely related to the Pb^{2+} vacancies and defect complexes.

Acknowledgements

Authors are grateful to Jianquan Qi and Ningxin Zhang for their help and valuable discussion.

References

- [1] Y. Hamata, H. Takuchi, K. Zomura, Jpn. Patent No. 63-280401, 1988.
- [2] D.J. Wang, Z.L. Gui, L.T. Li, Preparation and electrical properties of semiconducting strontium lead titanate PTCR ceramics, *J. Mater. Sci.: Mater. in Electronics* 8 (1997) 271–276.
- [3] Lu. Yuh-Yih, Tseng. Tseung-Yuen, Electrical characteristics of $(\text{Pb,Sr})\text{TiO}_3$ positive temperature coefficient ceramics, *Mater. Chem. Phys.* 53 (1998) 132–137.
- [4] Lee. Chengkuo, Lin. I.-Nan, Hu. Chen-Ti, Evolution of microstructure and V-shaped positive temperature coefficient of resistivity of $(\text{Pb}_{0.6}\text{Sr}_{0.4})\text{TiO}_3$ materials, *J. Am. Ceram. Soc.* 77 (5) (1994) 1340–1344.
- [5] W. Heywang, Barium titanate als sperrschichtbleiter, *Solid State Electronics* 44 (3) (1961) 51–58.
- [6] S. Iwaya, H. Masumura, H. Taguchi, M. Hamada, *J. Electron. Ceram. Jpn.* 19 (1988) 33.
- [7] D.J. Wang, J. Qiu, Y.C. Guo, Z.L. Gui, T.L. Li, Grain boundary effects in NTC-PTC composite thermistor materials, *J. Mater. Res.* 14 (1) (1999) 120–123.
- [8] Hsiu-Fung Cheng, Chen-Ti Hu, Yen-Yi Lin, et al., Modeling on the resistivity-temperature properties of $(\text{Pb}_{0.6}\text{Sr}_{0.4})\text{TiO}_3$ materials prepared by the rapid thermal sintering process, *Jpn. J. Appl. Phys.* 37 (1998) 1932–1938.
- [9] Chen-Chia Chou, Hon-Yi Chang, I-Nan Lin, et al., Microscopic examination of the microwave sintered $(\text{Pb}_{0.6}\text{Sr}_{0.4})\text{TiO}_3$ positive-temperature-coefficient resistor materials, *Jpn. J. Appl. Phys.* 37 (1998) 5269–5272.
- [10] D.J. Wang, Z.L. Gui, L.T. Li, Preparation and electrical properties of semiconducting strontium-lead titanate PTCR ceramics, *J. Mater. Sci.: Mater. in Electronics* 8 (1997) 271–276.
- [11] Horng-Yi Chang, Kuo-Shung Liu, Chen-Ti Hu, et al., Electrical properties of microwave-sintered $(\text{Sr}_{0.4}\text{Pb}_{0.6})\text{TiO}_3$ ceramics, *Jpn. J. Appl. Phys.* 35 (1996) 656–662.